Electronic Supplementary Material (ESI) for Inorganic Chemistry Frontiers.
This journal is © the Partner Organisations 2019

Table S1. Fractional atomic coordinates and isotropic or equivalent isotropic displacement parameters (Å^2) of $K_3BiTaP_3O_{13}$.

	x	*y*	*z*	U_{iso}*/U_{eq}
K1	0.40010 (11)	0.28034 (10)	−0.250000	0.0253 (4)
K2	0.666667	0.333333	0.500000	0.0280 (6)
K3	0.000000	0.000000	0.000000	0.0297 (9)
Bi1	0.22163 (2)	0.22163 (2)	0.250000	0.01002 (9)
Ta1	0.500000	0.500000	0.000000	0.00884 (9)
P1	0.46274 (11)	0.32463 (10)	0.250000	0.0118 (3)
P2	0.18109 (13)	0.18109 (13)	−0.250000	0.0119 (4)
O1	0.4739 (3)	0.3834 (2)	0.0776 (5)	0.0343 (10)
O2	0.5288 (3)	0.2972 (3)	0.250000	0.0300 (13)
O3	0.3712 (3)	0.2495 (3)	0.250000	0.0460 (19)
O4	0.2327 (3)	0.2327 (3)	−0.0784 (7)	0.0351 (13)
O5	0.1678 (4)	0.0894 (4)	−0.250000	0.0410 (15)
O6	0.5432 (3)	0.5432 (3)	0.250000	0.0109 (12)

Table S2. Atomic anisotropic displacement parameters (Å^2) of $K_3BiTaP_3O_{13}$.

	U^{11}	U^{22}	U^{33}	U^{12}	U^{13}	U^{23}
K1	0.0251 (8)	0.0153 (7)	0.0385 (9)	0.0125 (7)	0.000	0.000
K2	0.0243 (8)	0.0243 (8)	0.0354 (15)	0.0122 (4)	0.000	0.000
K3	0.0330 (14)	0.0330 (14)	0.023 (2)	0.0165 (7)	0.000	0.000
Bi1	0.01032 (13)	0.01032 (13)	0.00958 (15)	0.00528 (13)	0.000	0.000
Ta1	0.01051 (13)	0.01051 (13)	0.00561 (14)	0.00535 (14)	0.00057 (11)	0.00057 (11)
P1	0.0128 (8)	0.0087 (7)	0.0135 (7)	0.0050 (6)	0.000	0.000
P2	0.0128 (8)	0.0128 (8)	0.0108 (10)	0.0069 (9)	0.000	0.000
O1	0.073 (3)	0.0152 (17)	0.0127 (16)	0.020 (2)	−0.0137 (18)	−0.0029 (14)
O2	0.016 (3)	0.022 (3)	0.055 (4)	0.011 (2)	0.000	0.000
O3	0.012 (3)	0.010 (3)	0.113 (6)	0.003 (2)	0.000	0.000
O4	0.034 (2)	0.034 (2)	0.015 (2)	0.000 (3)	−0.0016 (18)	−0.0016 (18)
O5	0.058 (4)	0.029 (3)	0.054 (4)	0.035 (3)	0.000	0.000
O6	0.011 (2)	0.011 (2)	0.009 (3)	0.005 (3)	0.000	0.000

Table S3. Select bond distances of $K_3BiTaP_3O_{13}$.

K1—O3^{i}	2.597 (5)	K3—O5^{xvii}	3.134 (5)
K1—O6^{ii}	2.769 (5)	K3—O5^{xviii}	3.134 (5)
K1—O2^{i}	2.818 (5)	Bi1—O5^{vi}	2.225 (5)
K1—O1	2.846 (4)	Bi1—O5^{xi}	2.225 (5)
K1—O1^{iii}	2.846 (4)	Bi1—O4^{xix}	2.345 (5)
K1—O4	2.919 (4)	Bi1—O4	2.345 (5)
K1—O4^{iii}	2.919 (4)	Bi1—O3^{xx}	2.445 (5)
K2—O2^{iv}	2.827 (4)	Bi1—O3	2.445 (5)
K2—O2^{v}	2.827 (4)	Ta1—O6^{ii}	1.937 (2)

K2—O2^{vi}	2.827 (4)	Ta1—O6	1.937 (2)
K2—O2^{vii}	2.827 (4)	Ta1—O1^{ii}	1.961 (3)
K2—O2	2.827 (4)	Ta1—O1^{xxi}	1.961 (3)
K2—O2^{viii}	2.827 (4)	Ta1—O1^{xxii}	1.961 (3)
K3—O5	3.134 (5)	Ta1—O1	1.961 (3)
K3—O5^{vi}	3.134 (5)	P1—O2	1.477 (5)
K3—O5^{ix}	3.134 (5)	P1—O3	1.501 (5)
K3—O5^{x}	3.134 (5)	P1—O1	1.557 (3)
K3—O5^{xi}	3.134 (5)	P1—O1^{xix}	1.557 (3)
K3—O5^{xii}	3.134 (5)	P2—O5	1.523 (6)
K3—O5^{xiii}	3.134 (5)	P2—O5^{xvii}	1.523 (6)
K3—O5^{xiv}	3.134 (5)	P2—O4^{iii}	1.526 (5)
K3—O5^{xv}	3.134 (5)	P2—O4	1.526 (5)
K3—O5^{xvi}	3.134 (5)		
O6^{ii}—Ta1—O6	180.0	O1^{xxii}—Ta1—O1	89.6 (3)
O6^{ii}—Ta1—O1^{ii}	89.85 (15)	O2—P1—O3	113.1 (3)
O6—Ta1—O1^{ii}	90.15 (15)	O2—P1—O1	111.4 (2)
O6^{ii}—Ta1—O1^{xxi}	90.15 (15)	O3—P1—O1	108.3 (2)
O6—Ta1—O1^{xxi}	89.85 (15)	O2—P1—O1^{xix}	111.4 (2)
O1^{ii}—Ta1—O1^{xxi}	89.6 (3)	O3—P1—O1^{xix}	108.3 (2)
O6^{ii}—Ta1—O1^{xxii}	89.85 (15)	O1—P1—O1^{xix}	103.9 (3)
O6—Ta1—O1^{xxii}	90.15 (15)	O5—P2—O5^{xvii}	104.5 (5)
O1^{ii}—Ta1—O1^{xxii}	90.4 (3)	O5—P2—O4^{iii}	111.54 (16)
O1^{xxi}—Ta1—O1^{xxii}	180.00 (8)	O5^{xvii}—P2—O4^{iii}	111.54 (16)
O6^{ii}—Ta1—O1	90.15 (15)	O5—P2—O4	111.54 (16)
O6—Ta1—O1	89.85 (15)	O5^{xvii}—P2—O4	111.54 (16)
O1^{ii}—Ta1—O1	180.0	O4^{iii}—P2—O4	106.3 (4)
O1^{xxi}—Ta1—O1	90.4 (3)		
Symmetry codes: (i) *x*, *x*−*y*, *z*−1/2; (ii) −*x*+1, −*y*+1, −*z*; (iii) *x*, *y*, −*z*−1/2; (iv) −*x*+*y*+1, *y*, *z*+1/2; (v) −*y*+1, *x*−*y*, *z*; (vi) *x*, *x*−*y*, *z*+1/2; (vii) −*x*+*y*+1, −*x*+1, −*z*+1/2; (viii) −*y*+1, −*x*+1, *z*+1/2; (ix) −*x*, −*x*+*y*, −*z*−1/2; (x) −*x*+*y*, −*x*, −*z*−1/2; (xi) *x*−*y*, *x*, *z*+1/2; (xii) *y*, −*x*+*y*, −*z*; (xiii) −*y*, *x*−*y*, *z*; (xiv) −*x*+*y*, *y*, *z*+1/2; (xv) *x*−*y*, −*y*, −*z*−1/2; (xvi) −*y*, −*x*, *z*+1/2; (xvii) *y*, *x*, −*z*−1/2; (xviii) −*x*, −*y*, −*z*; (xix) *x*, *y*, −*z*+1/2; (xx) *y*, *x*, −*z*+1/2; (xxi) *y*, *x*, *z*; (xxii) −*y*+1, −*x*+1, −*z*.			

Table S4. The state energies (eV) of the lowest conduction band (L–CB) and the highest valence band (H–VB) at some k-points of $K_3BiTaP_3O_{13}$.

k-point	G(0,0,0)	A(0,0,1/2)	H(-1/3,2/3,1/2)	K(-1/3,2/3,0)	G(0,0,0)	M(0,1/2,0)	L(0,1/2,1/2)	H(-1/3,2/3,1/2)
L–CB	4.164	4.908	4.853	4.164	4.164	4.164	4.853	4.853
H–VB	-0.372	0.000	-0.005	-0.332	-0.372	-0.321	-0.002	-0.005

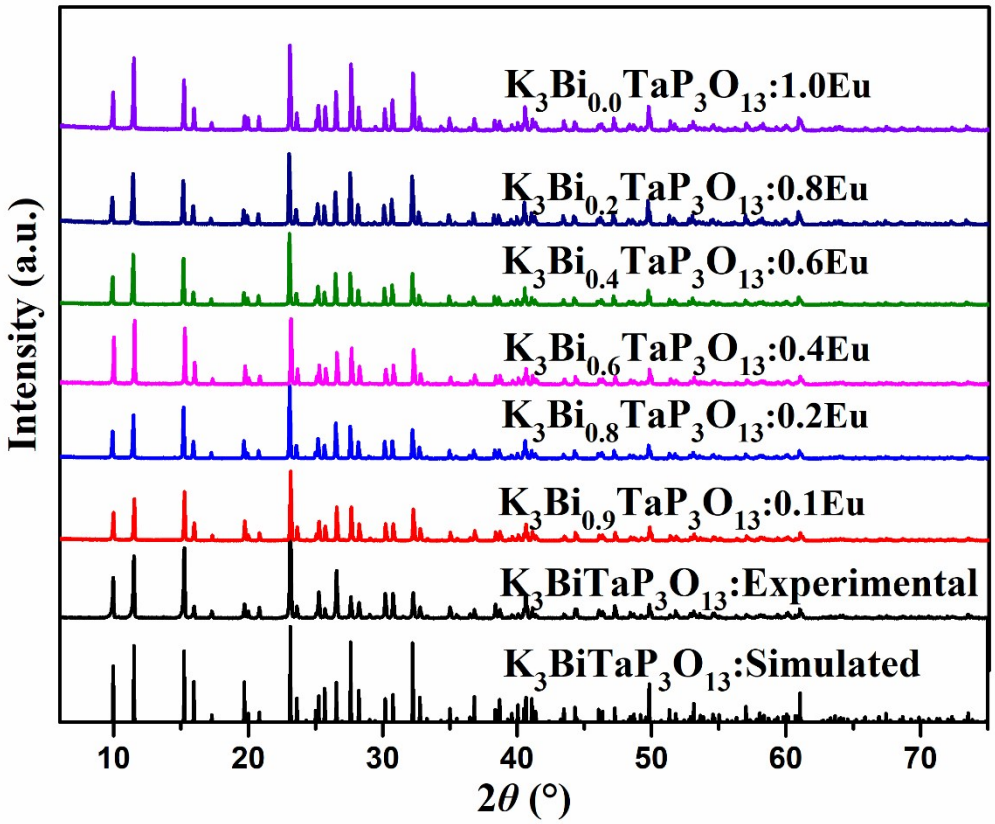

Figure S1. Simulated X-ray powder diffraction pattern of $K_3BiTaP_3O_{13}$ and experimental X-ray powder diffraction patterns of $K_3Bi_{1-x}TaP_3O_{13}$:*x*Eu (x=0─1) in the 2θ range of 6─75°.

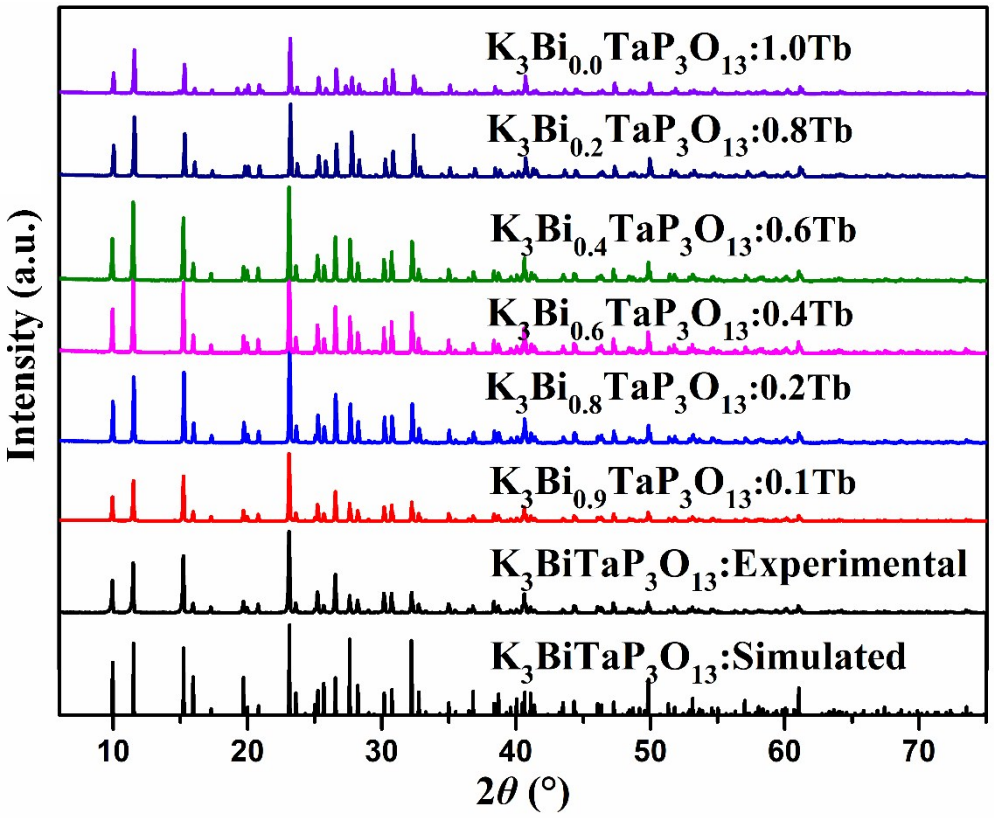

Figure S2. Simulated X-ray powder diffraction pattern of $K_3BiTaP_3O_{13}$ and experimental X-ray powder diffraction patterns of $K_3Bi_{1-x}TaP_3O_{13}$:*x*Tb (x=0─1) in the 2θ range of 6─75°.

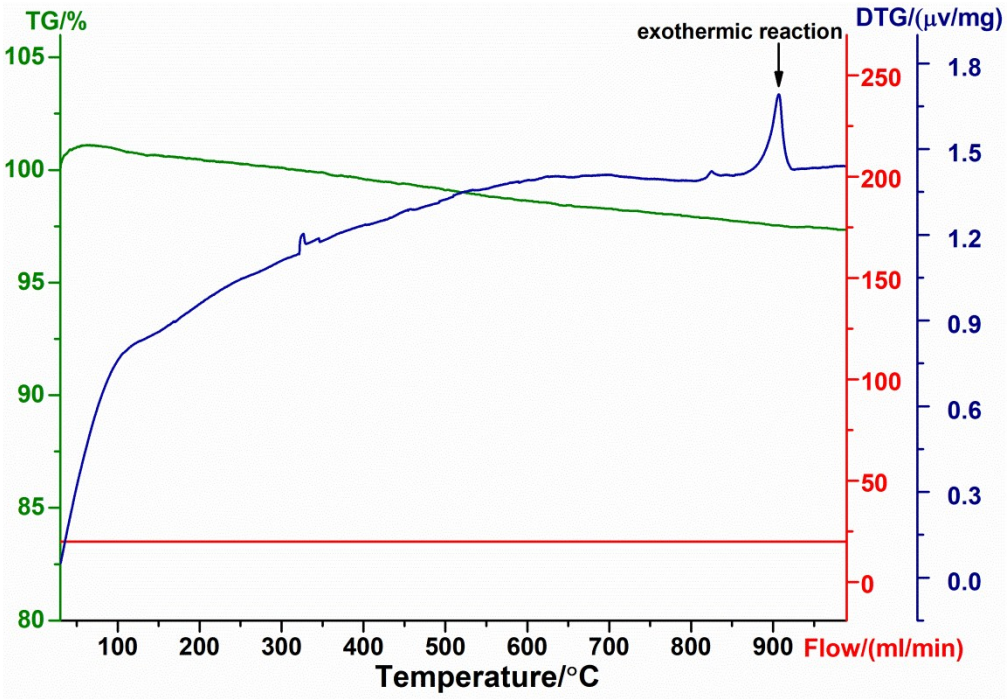

Figure S3. TG and DTA curves for $K_3BiTaP_3O_{13}$.

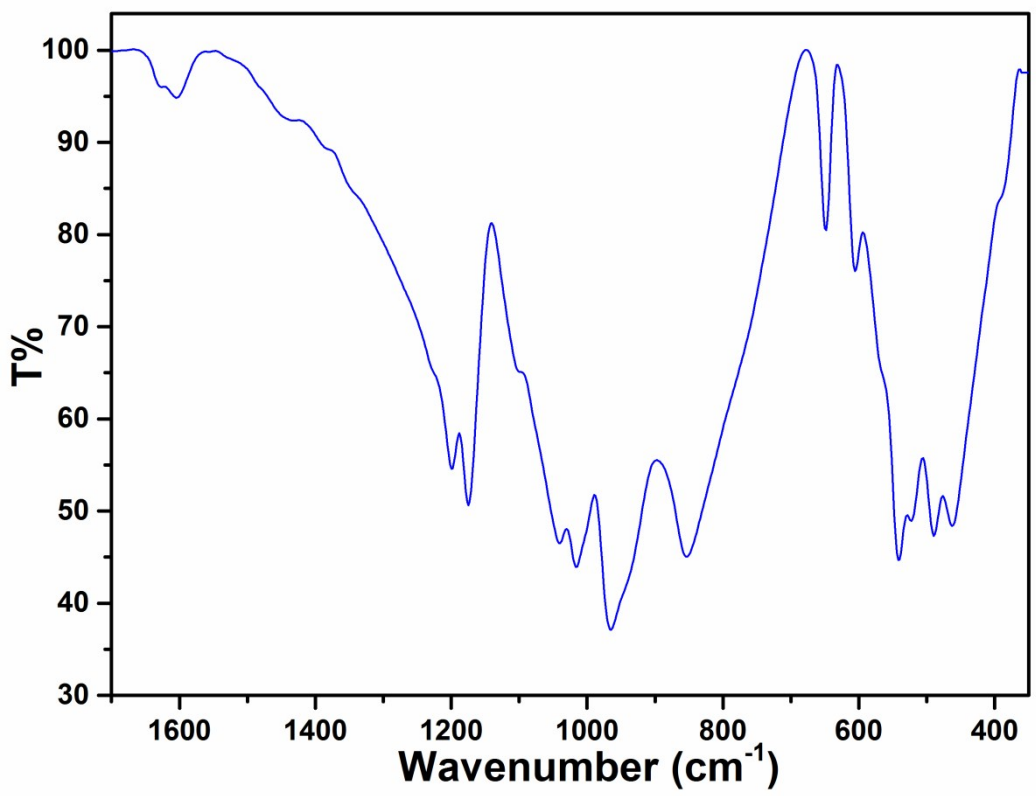

Figure S4. The IR spectra of orthophosphate $K_3BiTaP_3O_{13}$ in the range of 350─1700 cm^{-1}.

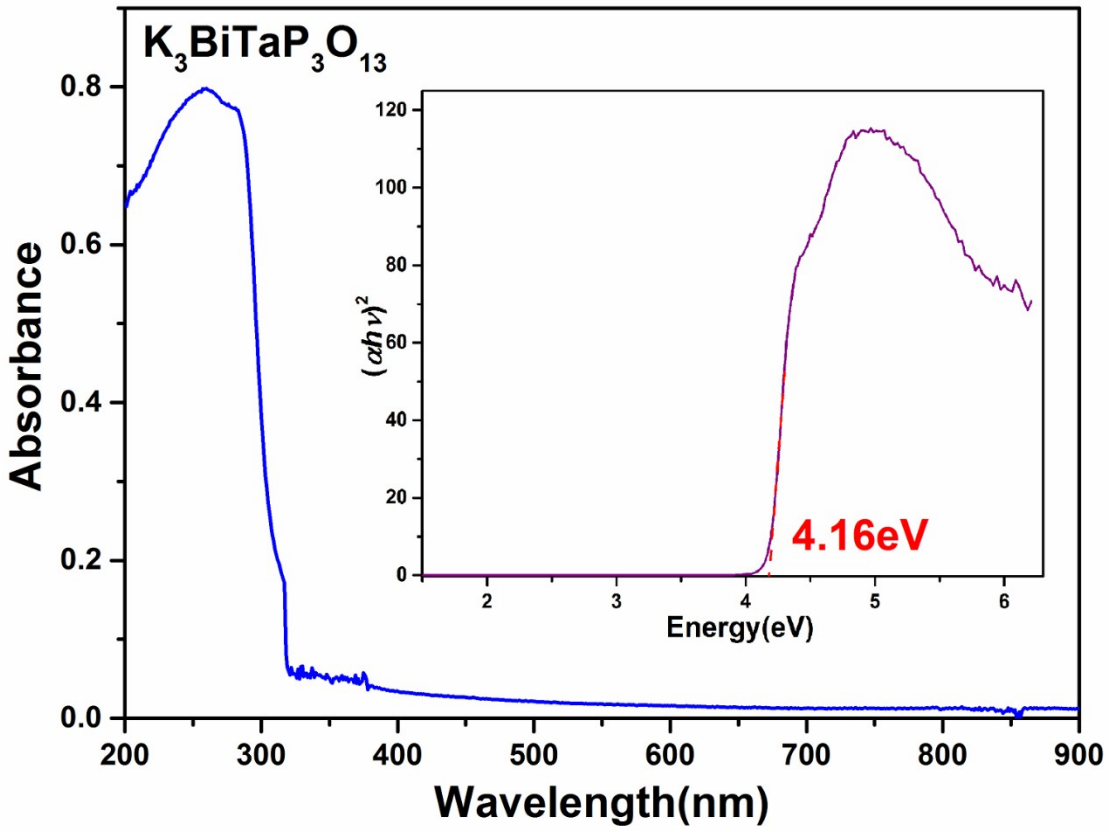

Figure S5. Experimental UV-vis absorption spectrum of $K_3BiTaP_3O_{13}$ ranging from 200 to 900 nm.

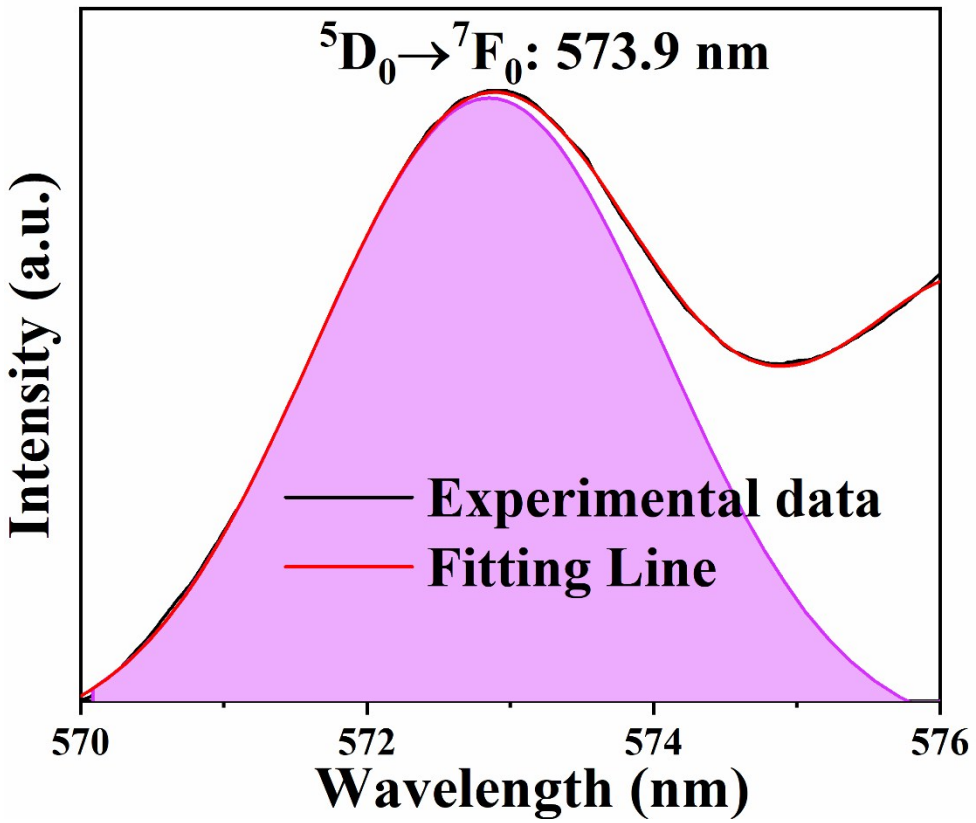

Figure S6. The emission spectrum of $K_3Bi_{0.6}Eu_{0.4}TaP_3O_{13}$ at 570−576 nm to present the $^5D_0 \rightarrow {}^7F_0$ band in high definition.

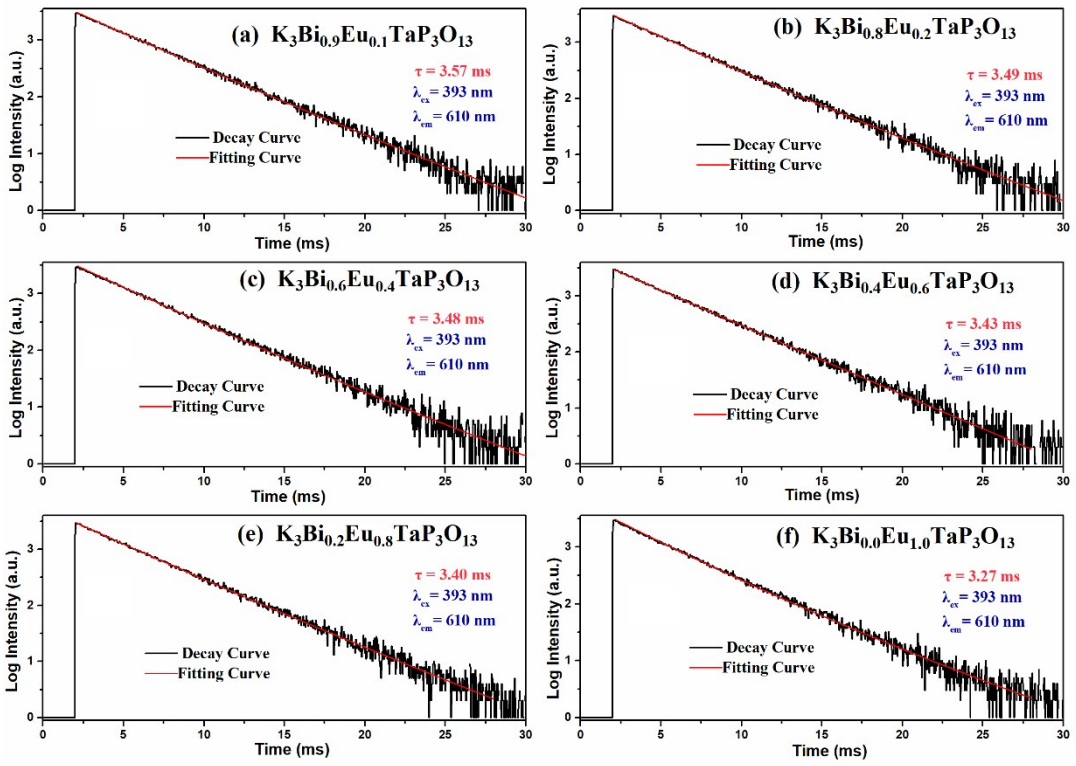

Figure S7. PL decay curves of the Eu^{3+} emission at 610 nm under 393 nm excitation for the phosphors $K_3Bi_{1-x}TaP_3O_{13}$:xEu^{3+} x = 0.1 (a), 0.2 (b), 0.4 (c), 0.6 (d), 0.8 (e) and 1.0 (f).

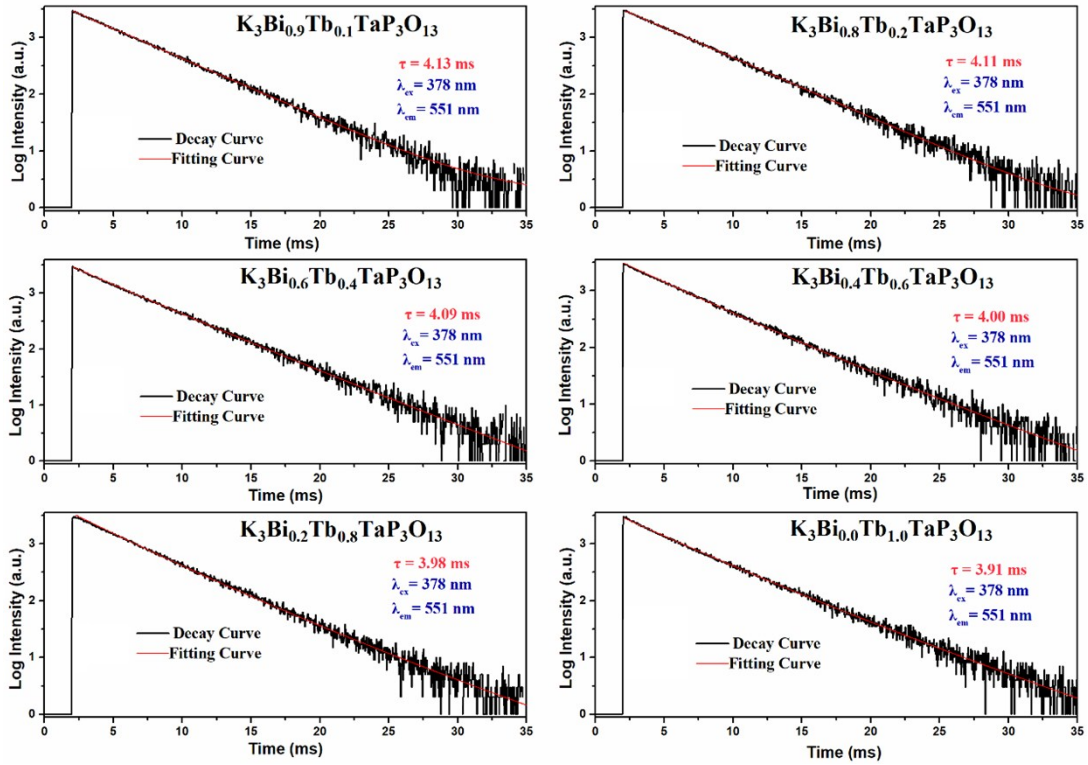

Figure S8. PL decay curves of the Tb^{3+} emission at 551 nm under 378 nm excitation for the phosphors $K_3Bi_{1-x}TaP_3O_{13}$:xTb^{3+} x = 0.1 (a), 0.2 (b), 0.4 (c), 0.6 (d), 0.8 (e) and 1.0 (f).

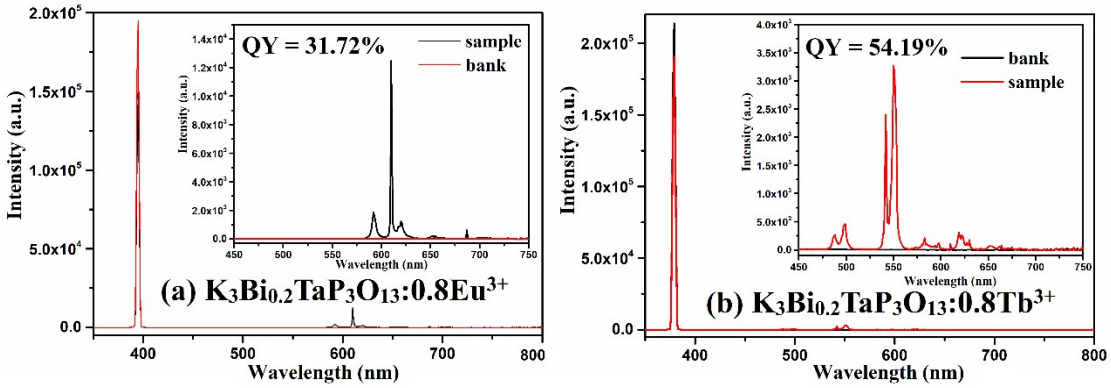

Figure S9. The fluorescence quantum yield of $K_3Bi_{0.2}TaP_3O_{13}$:$0.8Eu^{3+}$ (a) excited by 393 nm and $K_3Bi_{0.2}TaP_3O_{13}$:$0.8Tb^{3+}$ (b) excited by 378 nm.